Catalytic conversion of carbohydrates into 5-ethoxymethylfurfural using γ-AlOOH and CeO₂@B₂O₃ catalyst synergistic effect†

Luxin Zhang, [ID] * Xu Xing, Ruijun Sun and Meng Hu

Selective catalytic conversion of carbohydrates to 5-ethoxymethylfurfural (EMF) is a critical approach to the biorefinery. In this work, solid acid catalysts of γ-AlOOH and CeO₂@B₂O₃ were used to convert carbohydrates to EMF in a one-pot process, performed in an ethanol/DMSO solvent system. The synergistic effect of γ-AlOOH and CeO₂@B₂O₃ was studied. Furthermore, the morpho-structural properties of the catalysts were characterized, and the effects of reaction time, reaction temperature, catalyst load, and the amount of cosolvent on the conversion of glucose to EMF were examined and optimized. Under the reaction conditions of 170 °C for 20 h, glucose, sucrose, cellobiose, inulin and starch were used as raw materials, and the EMF yield range was 9.2–27.7%. The results showed that the synergistic effect of γ-AlOOH and CeO₂@B₂O₃ further causes the combination of multiple acid sites with different types and strength distributions. Particularly, the collaboration between weak, medium-strong, and strong acid, as well as between Lewis and Brønsted acidity, is of great significance for EMF generation. The reusability experiments showed that the combined catalytic system was easily separated and maintained catalytic activity for five successive reactions without further intermediate regeneration steps. This work provides a promising route for the catalytic conversion of biomass-derived carbohydrates into EMF.

1. Introduction

Excessive dependence on fossil resources has led to severe environmental pollution, global warming and resource depletion, motivating the use of chemicals and fuels from renewable resources through clean synthetic routes and environmentally friendly processes.[1,2] As the only renewable organic carbon source, biomass is considered as the most potential raw material to produce value-added chemicals, and to replace fossil resources.[3,4] Conversion of biomass-derived carbohydrates into platform compounds or other fine chemicals effectively utilizes the carbon resources in biomass.[5,6]

5-ethoxymethylfurfural (EMF), as a representative of the 5-alkoxymethylfurfural ether family, has the advantages of high energy density (8.7 kW h L^{-1}), high cetane number, high boiling point (508 K), low toxicity, and good fluidity at low temperature and can dramatically decrease sulfur dioxide and fine particle matter emissions.[7–10] Generally, EMF can be obtained by the single-step etherification of 5-hydroxymethylfurfural (HMF), the two-step dehydration-etherification cascade reaction of fructose, the three-step isomerization–dehydration–etherification cascade reaction of glucose, or synthesis from lignocellulosic biomass materials.[11,12] Among these, using HMF or fructose as raw materials to produce EMF can obtain relatively high yields. For example, Yuan *et al.* used Fe₃O₄@C–SO₃H to synthesize EMF, with yields of 88.4% and 67.8% obtained from HMF and fructose, respectively.[4] Nonetheless, owing to the high cost, it could be unfeasible to use HMF or fructose as raw materials in large-scale industrial production.[13–15] In contrast, glucose, as the monomer unit of cellulose and the least expensive hexose, could be considered the preferred raw material for EMF preparation due to its abundance and availability.[16,17]

The multiple cascade reaction pathway of EMF synthesis from glucose is detailed in Scheme 1. Currently, the three-step isomerization–hydrolyzation–etherification cascade reaction pathway of glucose is generally accepted.[12,18] Specifically, the formation of EMF requires the etherification of HMF, and the formation of HMF requires the isomerization of glucose to fructose, which is then further dehydrated.[19,20] Simultaneously, another parallel generation pathway of EMF is glucose to ethyl glucoside (EG), isomerization of EG to ethyl fructoside (EF), and then the resulting EMF reaction route. In different steps of the three-step reaction strategy, the operation is very complicated if the intermediate products are separated, increasing the cost and hindering the large-scale production. Furthermore, since

College of Environmental and Municipal Engineering, Shaanxi Key Laboratory of Environmental Engineering, Key Lab of Northwest Water Resource, Environment and Ecology, MOE, Xi'an University of Architecture and Technology, Xi'an 710055, P. R. China. E-mail: zhangluxinxx@126.com; Fax: +86 29 82205652; Tel: +86 29 82205652

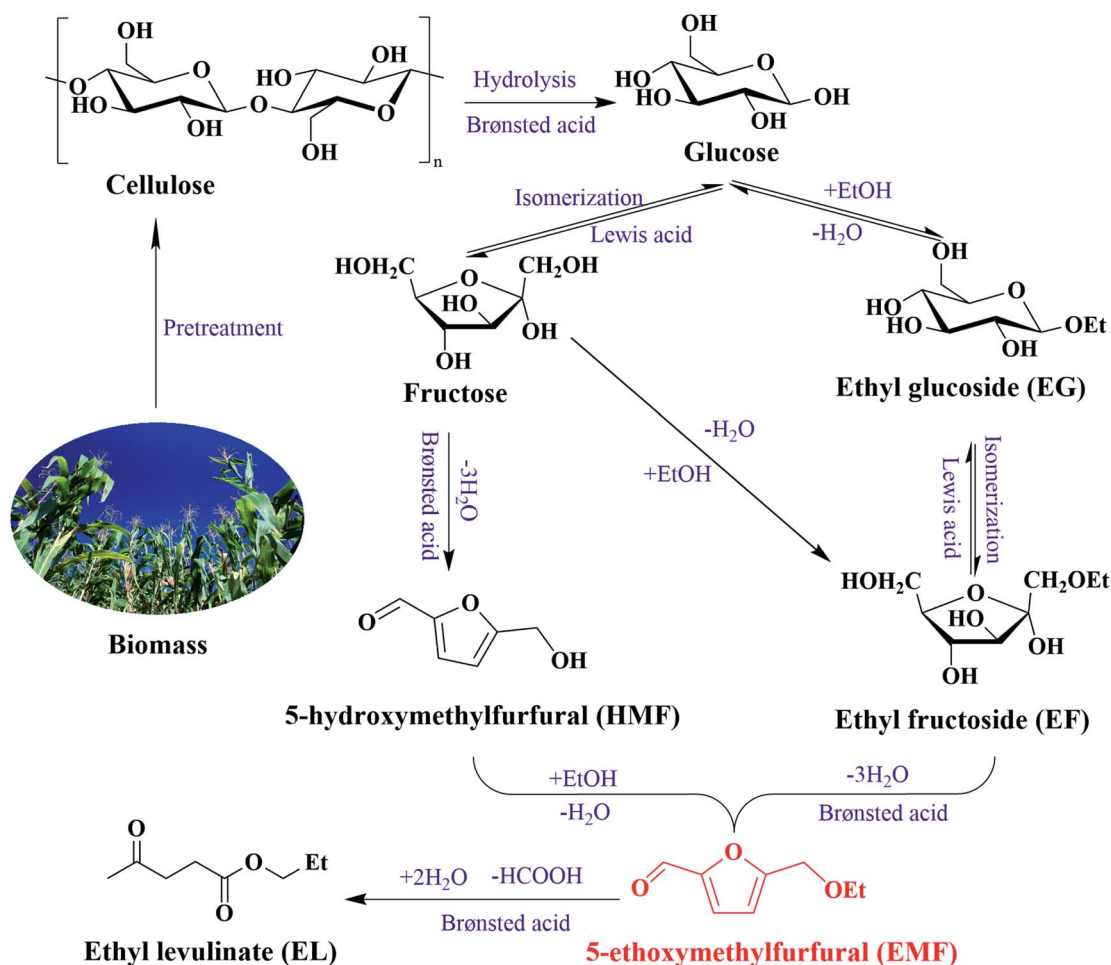† Electronic supplementary information (ESI) available. See https://doi.org/10.1039/d2ra01866g

the three steps in the route are all acid-catalyzed reactions, it is logical to integrate them into a one-pot reaction.[21] In this way, selectivity and recovery of acidic catalysts are the main issues to be considered. Homogeneous acid catalysts have been proved to be highly efficient on etherification and dehydration.[22] Nevertheless, the use of homogeneous acids has inherent disadvantages such as toxicity, corrosion of the equipment, many waste by-products and difficult separation.[23,24]

So far, various solid catalysts have been investigated for the one-pot synthesis of EMF from glucose, such as GO,[25] Lys/PW(2),[26] and USY.[27] However, regrettably, most catalytic systems have low yields, which could be attributed to the high stability of the six-membered pyranoside structure of glucose and low enolization degree.[2,28] For example, Liu *et al.* reported an approach to synthesizing EMF from glucose with MIL-101-SO$_3$H by reacting at 100 °C for 15 hours in an ethanol-THF solvent system, with a relatively low EMF yield (<10%).[29] In multiple parallel and cascade reactions for the efficient production of EMF from glucose, isomerization from glucose to fructose and the isomerization from EG to EF are the key rate-limiting steps.[19] The isomerization of glucose may need to go through two reaction steps, namely enolation reaction and 1,2-H transfer reaction step. According to previous studies, Lewis acid

could be considered as the crux to break the isomerization equilibrium, and Brønsted acid is conducive to dehydration.[30] Furthermore, the etherification reaction depends on the synergistic effect of Lewis acid and Brønsted acid.[31] Thereupon, catalysts containing Lewis and Brønsted acid bifunctional active sites may catalyze more efficiently the conversion of carbohydrates containing glucose units to EMF.[32] In addition, due to the complexity of the cascade reaction steps, each step requires different acidic sites and strengths. The strength distribution of different types of acid sites is also an essential factor affecting EMF yield. Generally speaking, a weak acid catalyst is more conducive to promoting the dehydration reaction while reducing the furan ring-opening to improve the yield of EMF, especially the weak Brønsted acid in the dehydration reaction showed an enhanced catalytic effect. Compared with Brønsted acid, solid catalysts with strong Lewis acid sites have higher catalytic activity in isomerization reactions.[33] Up to now, the development of a combined catalyst system with different types and strength distributions of acid sites for the one-pot conversion of carbohydrates to EMF remained an emerging challenge.[34,35]

Aluminum and its compounds are widely used in solid Lewis acid catalysts. Boehmite, an abundant and inexpensive

Scheme 1 Reaction pathways of biomass to EMF.

aluminium oxide hydroxide, has weak Lewis acid sites, and the number of Lewis acid sites can be adjusted with different preparation conditions.[36] Moreover, ceria-based materials, especially cerium dioxide, are widely used in chemical reactions due to their specific acid activity. The synthesis of $CeO_2@B_2O_3$ by complex boron oxides can effectively enhance the acidity of cerium dioxide and improve the catalytic activity. The number and strength of acid sites can also be changed by preparation conditions to improve the activity of the materials.

Considering these aspects, in the present work, an environmentally friendly, efficient, and sustainable method was developed to convert biomass-derived carbohydrates into high value-added product EMF. The synergistic catalytic system of solid acid catalysts γ-AlOOH and $CeO_2@B_2O_3$ has been synthesized. This system can integrate the cascade catalytic steps into one pot and has the advantages of easy preparation and low corrosion. Particularly, the distribution of products can be optimized by adjusting the acid sites, improving the selectivity and efficiency of the catalyst. The microstructure, physicochemical properties, and acidic properties of the catalysts were investigated. The influence factors, including catalyst loading, reaction temperature, and reaction time, especially the ratio of different catalysts, were meticulously examined. The recyclability of the catalyst was investigated by a reusability experiment.

2. Materials and methods

2.1. Chemicals and materials

Glucose (99%), concentrated ammonia water and cerium nitrate hexahydrate ($Ce(NO_3)_3·6H_2O$) were purchased from Aladdin Industrial Corporation (Shanghai, China). Anhydrous ethanol (AR grade, 99.7%) was acquired from Tianli Chemical Reagent Co., Ltd. (Tianjin, China). The chemicals include dimethyl sulfoxide (DMSO, 99%), aluminium nitrate non-ahydrate ($Al(NO_3)_3·9H_2O$), boric acid and ammonium bicarbonate were provided by Tianjin Kemiou Chemical Reagent Co. Ltd. (Tianjin, China). Sigma-Aldrich supplied all the other reagents and chemicals, which were used as received without further purification unless otherwise stated.

2.2. Catalyst preparation

The synthesis of boehmite (γ-AlOOH) was performed as follows: aluminium nitrate nonahydrate ($Al(NO_3)_3·9H_2O$, 15 mmol) and ammonium bicarbonate (NH_4HCO_3, 30 mmol) were dissolved in 50 mL deionized water under stirring until the solution became transparent. In the next step, the pH was adjusted to 9.0 with concentrated ammonia water. Then, the solution was transferred to a 100 mL Teflon-lined stainless reaction kettle and heated at 150 °C for 12 h. After cooling to room temperature, the mixture was centrifuged and washed with deionized water and dried at 150 °C for 12 h.

$CeO_2@B_2O_3$ was prepared by the following method: 18.9 g $Ce(NO_3)_3·6H_2O$ and 0.676 g boric acid were mixed and dissolved in 50 mL ethanol, and stirred at room temperature until it was completely dissolved. The ethanol in the mixture was then evaporated by vacuum distillation, resulting in a thick, gelatinous colorless substance that was cooled and dried at room temperature to form a white solid substance. Subsequently, the obtained solid material was ground evenly and placed in the tube furnace. The airflow rate was set at 50 mL min^{-1}, the heating rate was set at 5 °C min^{-1}, and the temperature was kept at 600 °C for 4 h to obtain the yellow solid material $CeO_2@B_2O_3$.

2.3. Conversion of glucose into EMF

In a typical run of glucose conversion to EMF, the first step was to add 20 mg of glucose, 5 mg of γ-AlOOH, 5 mg of $CeO_2@B_2O_3$, and solvent (0.3 mL DMSO, 1.7 mL ethanol) into a 15 mL thick wall pressure-resistant glass reactor. Then the reactor was placed in a preheated oil bath at the set temperature (170 °C) with continuous magnetic stirring and reacted for a desirable time (20 h). The reaction vessel was rapidly cooled by running water when the reaction was completed. Subsequently, the resulting reaction mixture was filtered and diluted for EL/HMF/EMF analysis. EL was analyzed by gas chromatography, HMF/EMF were analyzed by ultra-high-performance liquid chromatography (UHPLC). Details of these analyses are provided in ESI Appendix, Materials and Methods.†

The product yield was determined and calculated according to the following formula:

$$\text{Product yield } (\%) = \frac{\text{moles of product produced}}{\text{moles of initial glucosyl units in the feedstock}} \times 100\%$$

3. Results and discussion

3.1. Characterization of catalyst

SEM images of γ-AlOOH and $CeO_2@B_2O_3$ are depicted in Fig. S1.† Among them, the particle size of $CeO_2@B_2O_3$ is mainly distributed between 100–250 nm. The agglomeration of catalyst particles forms an irregular spatial structure with a rough surface. Catalyst γ-AlOOH shows a bulk structure with slit pores.

The XRD patterns of the prepared catalysts are shown in Fig. 1. Typical diffraction peaks can be observed around 2θ angles of 28.46°, 33.04°, 47.38°, 56.29°, 59.05°, 69.41°, 76.72° and 79.08°. These diffraction peaks belong to the (111), (200), (220), (311), (222), (400), (331) and (420) diffraction crystal planes of the cubic crystal system CeO_2 (JCPDS 078-0694), which is the characteristic pattern of typical CeO_2. Furthermore, it is remarkable that no diffraction lines of the B_2O_3 phase were observed in the XRD pattern of the sample $CeO_2@B_2O_3$, indicating that the B_2O_3 species may be amorphous state or highly dispersed.[37] Diffraction peaks appear near $2\theta = 14.27°$, 28.16°, 38.33°, 49.27°, 55.38°, 64.93° and 72.04°, which are consistent with the pattern of orthogonal-crystal γ-AlOOH (JCPDS 021-1307) markers by comparison with the standard diffraction patterns. The crystal faces corresponding to these characteristic peaks are (020), (120), (031), (200), (151), (002), and (171),
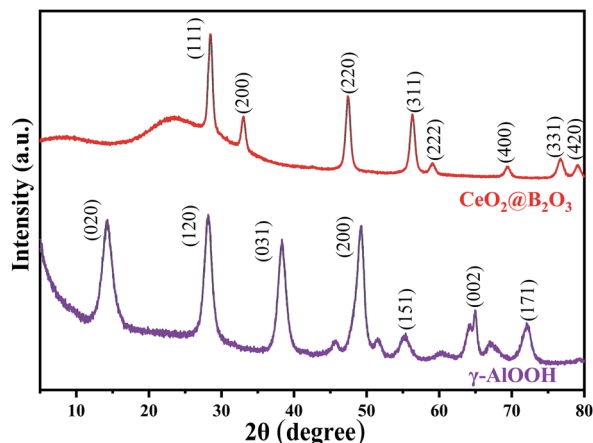
Fig. 1 X-ray diffraction patterns of $CeO_2@B_2O_3/\gamma\text{-AlOOH}$.

respectively.[38] The characteristic peaks were thin and sharp, which demonstrated that the products were high purity γ-AlOOH. At the same time, no diffraction peaks of impurities or other substances were observed.

XPS was used to detect γ-AlOOH and $CeO_2@B_2O_3$ and to determine further the surface element composition and

chemical state of the solid acid catalyst. As shown in Fig. 2(c), the binding energy position corresponding to the XPS spectra of B 1s is 191.7 eV, which may be related to the B–O–B bond in B_2O_3. The B element in the samples is composed of triangular and tetrahedral B–O coordination.[39] In addition, as visible from Fig. 2(a) and (b), there are six distinct peaks in the Ce 3d spectra corresponding to one state of Ce, and their corresponding binding energy positions from right to left are 882.7, 889.3, 898.6, 901.3, 907.5, 917.3 eV, respectively. Among them, the characteristic peaks of Ce^{4+} appear near 882.7 eV and 898.6 eV, which are close to the binding energies corresponding to the spectral peaks of Ce^{4+} $3d_{5/2}$ (882.4 eV) and Ce^{4+} $3d_{3/2}$ (903.9 eV), respectively.[40] More significantly, the unique satellite peak of CeO_2 appears at the binding energy of 917.3 eV. Moreover, there is no such peak in the Ce(III) spectrum, which also indicates that Ce exists in the valence state of Ce(IV). To determine the surface states of the γ-AlOOH, the XPS spectra with Al 2p peaks are shown in Fig. 2(d). As observed, the peak value of Al 2p appears at the binding energy of 74.6 eV. Thus, the dominating chemical state of aluminium atoms in the γ-AlOOH is Al(III). The uniform peak position indicates the stable existence of Al.[41]

The specific surface area, pore volume, and pore size distribution could affect the activity of the catalyst. The pore
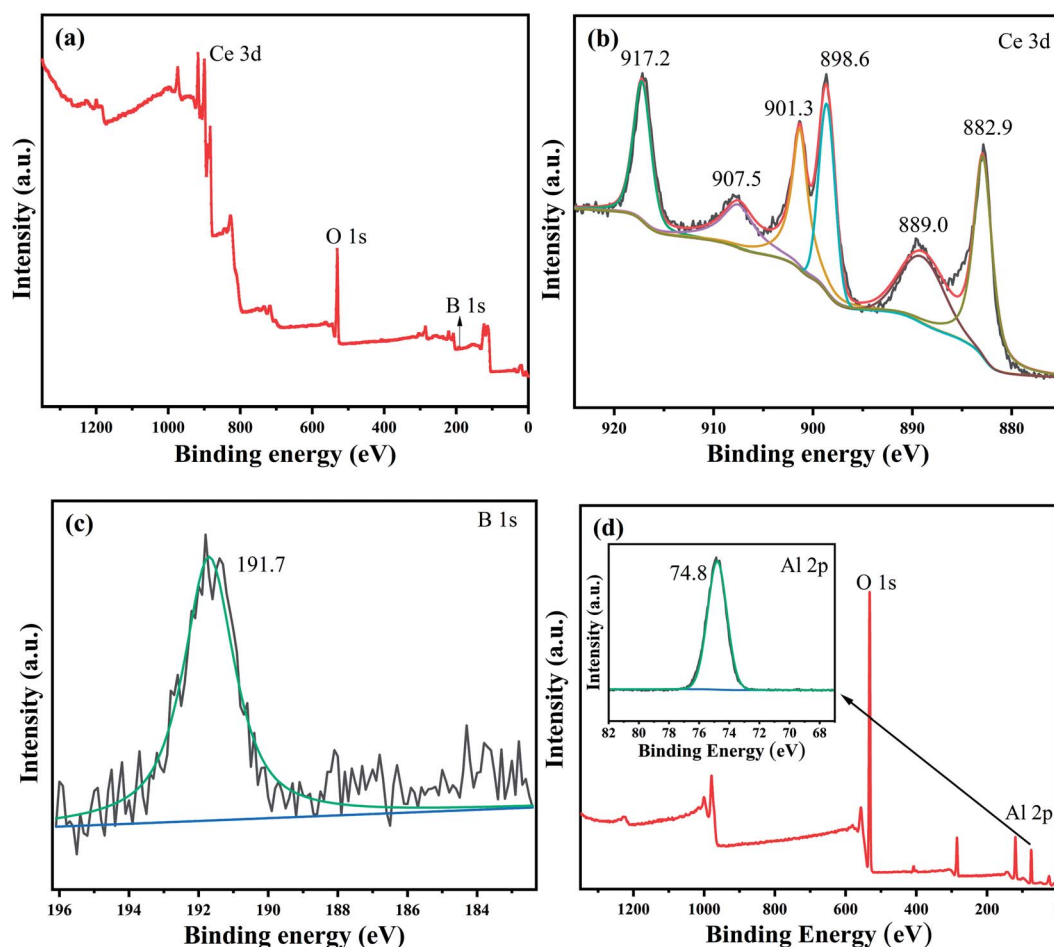

Fig. 2 XPS spectra of $CeO_2@B_2O_3/\gamma\text{-AlOOH}$ ((a) XPS survey spectrum of $CeO_2@B_2O_3$, (b) XPS spectra of Ce 3d, (c) XPS spectra of B 1s, (d) XPS survey spectrum of γ-AlOOH and XPS spectra of Al 2p).

Table 1 Acidity distribution of $CeO_2@B_2O_3/\gamma$-AlOOH

Catalyst	Weak acidity (mmol g^{-1})	Medium-strong acidity (mmol g^{-1})	Strong acidity (mmol g^{-1})
$CeO_2@B_2O_3$	0.08	0.25	0.03
γ-AlOOH	0.09	1.31	1.97

structure and specific surface area of catalysts $CeO_2@B_2O_3$ and γ-AlOOH were investigated by N_2 adsorption–desorption isotherms and pore size distribution curve (Fig. S2(a) and (b)†). As can be seen, the sorption isotherms of the catalyst belong to the IV type isotherms, as there are obvious mesoporous and hysteretic loops. Catalyst $CeO_2@B_2O_3$ has an H_1-type hysteresis loop between 0.8 and 0.9 relative pressures, indicating that the catalyst material is a spherical particle aggregate with a relatively uniform size. An H_2-type hysteresis loop appears in the medium pressure part of the γ-AlOOH catalyst, reflecting the complex pore structure and varying pore size. When the P/P_0 value is low, the adsorption mainly occurs on the surface and inner monolayer of the catalyst, and the adsorption amount slowly increases. When the P/P_0 value increases, capillary condensation occurs in the catalyst and the adsorption curve increases rapidly, then the adsorption curve and desorption curve are separated. The values of specific surface areas, pore volumes and pore sizes of $CeO_2@B_2O_3$ and γ-AlOOH catalysts are summarized in Table S1.† It has to be emphasized that the specific surface area of γ-AlOOH (176.7 m^2 g^{-1}) is much higher than that of catalyst $CeO_2@B_2O_3$ (22.4 m^2 g^{-1}).

Thermogravimetric (TG) analysis was used to investigate the thermal decomposition of the catalysts. As illustrated in Fig. S3(a),† the initial weight loss stage from 30–250 °C may be attributed to the loss of adsorbed water, and the continuous weight loss from 250–500 °C may be ascribed to the spontaneous reduction of Ce(IV) from CeO_2 to Ce(III) at high temperature.[42] As shown in Fig. S3(b),† the weight loss at 30–200 °C is due to the loss of free water molecules in the γ-AlOOH catalyst channels. Furthermore, most weight loss occurs above 200 °C, with a sharp loss $\approx$ 250 °C, which may account for the partial decomposition of γ-AlOOH to produce H_2O.[43]

NH_3-TPD analysis was used to investigate the surface acidity of $CeO_2@B_2O_3$ and γ-AlOOH catalysts. As demonstrated in Fig. S4(a),† there is an ammonia desorption peak around 100 °C, which corresponds to the weak acid sites on the surface of $CeO_2@B_2O_3$. Fig. S4(b)† shows a little desorption peak at 100–200 °C and a broader desorption peak at 500–700 °C, respectively, indicating the presence of weak and strong acid sites on the surface of γ-AlOOH. It can be observed that all samples showed a desorption peak at about 450 °C, which corresponds to the medium-strong acid sites on the surface. Table 1 lists the amount of acid at each acid level in the catalyst. The total amount of acid for $CeO_2@B_2O_3$ catalyst is 0.36 mmol g^{-1}, and that for the γ-AlOOH catalyst is 3.37 mmol g^{-1}.

To further prove Lewis and Brønsted acid sites types in the catalytic system, the Py-IR method was applied. Fig. 3(a), (b) and (c) show the Py-IR of the catalyst at 100 °C, 300 °C and 500 °C, respectively. The results showed that the bands at 1448 cm^{-1} and 1608 cm^{-1} indicated Lewis acid sites, while the bands at 1545 cm^{-1} and 1638 cm^{-1} corresponded to Brønsted acid sites, and the combined peak of Lewis and Brønsted acid sites appeared at 1490 cm^{-1}.[44] At the desorption temperatures of 100 °C, 300 °C and 500 °C, both Lewis and Brønsted acid sites were distributed, and the proportion and number of Lewis and Brønsted acid sites are collected in Table S2.†

3.2. Effect of different catalyst loading ratio on the conversion of glucose into EMF

As shown in Fig. 4, the catalyst loading ratio has a significant effect on the EMF yield. The activity of the dual-acid synergetic catalytic system was investigated in the reaction system of 20 mg glucose substrate, 1.7 mL anhydrous ethanol and 0.3 mL DMSO at 170 °C. When γ-AlOOH or $CeO_2@B_2O_3$ was used as catalyst alone, the yield of EMF from glucose alcoholysis was low. After combining them, the yield of EMF has been improved to varying degrees. Among them, under the combined catalysis of 5 mg γ-AlOOH and 5 mg $CeO_2@B_2O_3$, the maximum EMF yield reached 13.7% after 20 hours of reaction at 170 °C using an ethanol–DMSO solvent system. The EG yields declined with prolonging residence time upon all the combined mass ratio of γ-AlOOH and $CeO_2@B_2O_3$. As for HMF, an intermediate product to form EMF, the yield was low (<2%). The mass ratio of γ-AlOOH and $CeO_2@B_2O_3$ affects the distribution of different acid sites, thus affecting the acidic properties of the catalytic system and then the EMF yield and selectivity.
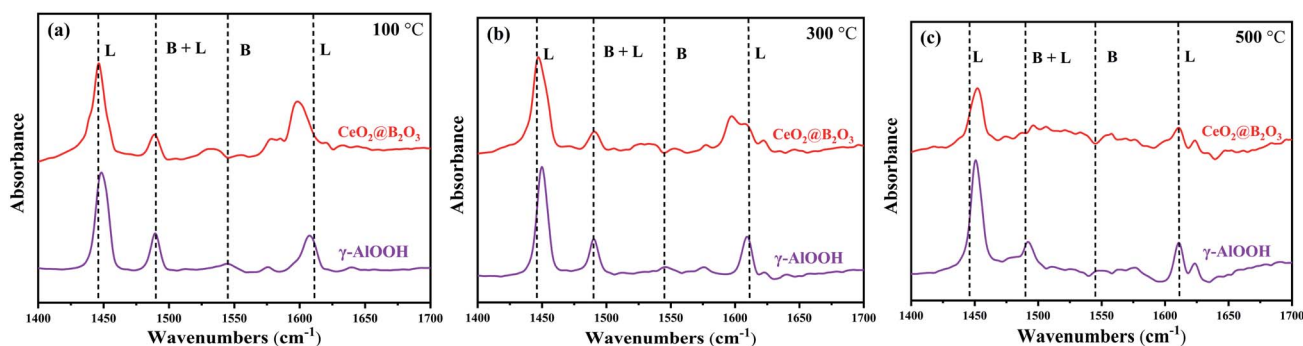

Fig. 3 Py-IR spectra of $CeO_2@B_2O_3/\gamma$-AlOOH ((a) desorption at 100 °C; (b) desorption at 300 °C; (c) desorption at 500 °C).
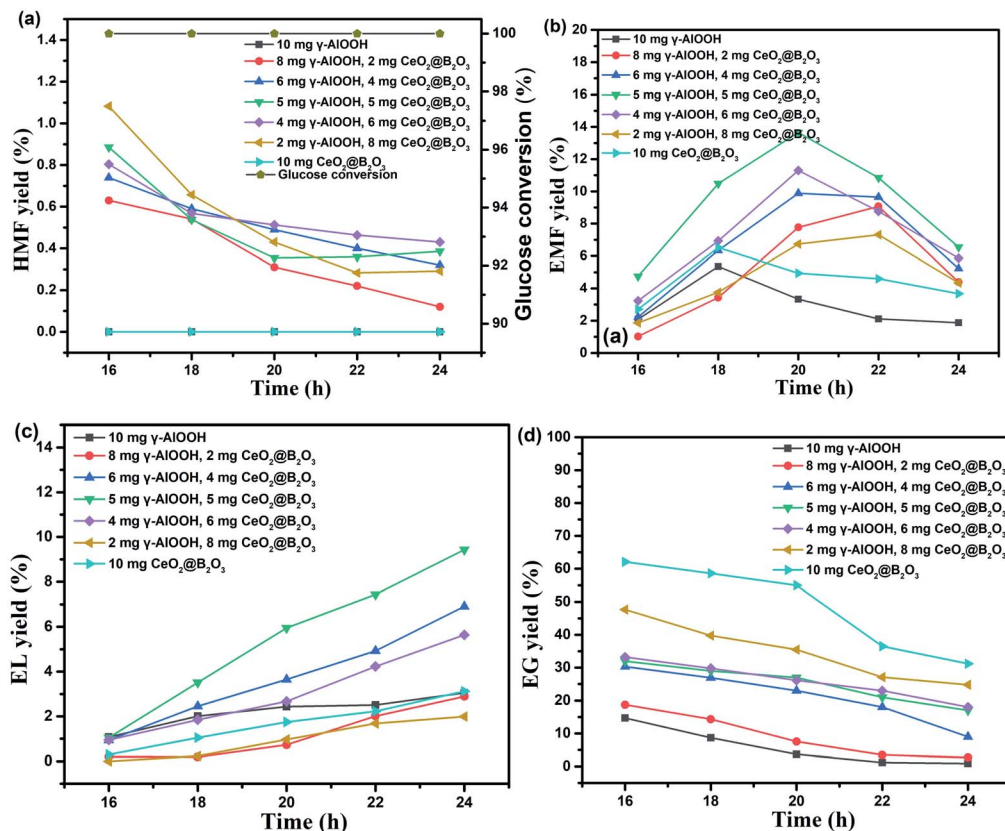
Fig. 4 Effect of catalyst loading on the conversion of glucose into EMF, (a) HMF yield, (b) EMF yield, (c) EL yield, (d) EG yield. Reaction conditions: 20 mg substrate, 1.7 mL ethanol, 0.3 mL DMSO, 170 °C.

In order to further study the synergistic effect of γ-AlOOH and $CeO_2@B_2O_3$ on the catalytic performance, the distribution of acid type, amount and strength of the catalytic system were changed by fine-tuning catalyst mass ratio (10 : 0, 8 : 2, 6 : 4, 5 : 5, 4 : 6, 8 : 2, 0 : 10, mg γ-AlOOH : mg $CeO_2@B_2O_3$). Tables 2 and 3 show the distribution of acid type, strength and amount of the paired γ-AlOOH and $CeO_2@B_2O_3$ catalysts with different mass ratio. "5 mg γ-AlOOH + 5 mg $CeO_2@B_2O_3$" reached the highest EMF yield (13.7%), further highlighting the importance of acid sites distribution in the glucose-to-EMF conversion. The total amount of acid on the catalyst was 3.37 mmol g^{-1} for γ-AlOOH and 0.36 mmol g^{-1} for $CeO_2@B_2O_3$, respectively. When the distribution of weak acid, medium-strong acid and strong acid was close to 1.00 : 9.18 : 11.76 (Table S4†), and Brønsted acid to Lewis acid ratio of 0.18 (Table S3†), the yield of EMF

reached the maximum mentioned above. This enhancement could be ascribed to the synergistic of γ-AlOOH and $CeO_2@B_2O_3$ under these specific acid sites ratio being more conducive to the isomerization of glucose to fructose and EG to EF. In parallel, the synergistic catalytic system can catalyze dehydration and subsequent etherification reaction more quickly, reduce the possibility of side reactions, and thus improve the EMF yield.

3.3. Effect of reaction temperature and time on the conversion of glucose into EMF

Under the synergistic catalysis of γ-AlOOH and $CeO_2@B_2O_3$, the optimal reaction temperature and time for synthesizing EMF from glucose alcoholysis was 170 °C and 20 h, respectively. As shown in Fig. 5, when the reaction temperature was elevated

Table 2 Influence of DMSO amount on EMF yield from glucose alcoholysis[a]

Entry	Reaction solvent	HMF yield/%	EL yield/%	EMF yield/%	EG yield/%
1	2.0 mL ethanol	0	0	0.5	34.2
2	1.7 mL ethanol, 0.3 mL DMSO	0.1	1.8	13.7	27.0
3	1.5 mL ethanol, 0.5 mL DMSO	0.1	3.4	21.8	19.6
4	1.3 mL ethanol, 0.7 mL DMSO	0.1	3.3	27.7	14.7
5	1.0 mL ethanol, 1.0 mL DMSO	0.9	2.7	17.6	8.4

[a] Reaction conditions: 20 mg substrate, 5 mg $CeO_2@B_2O_3$, 5 mg γ-AlOOH, 170 °C, 20 h.

Table 3 Investigations on EMF production yields from other carbohydrates

Entry	Substrate	Reaction conditions	HMF yield/%	EL yield/%	EMF yield/%
1[a]	Sucrose	170 °C, 20 h	0.1	4.9	13.6
2[a]	Inulin	170 °C, 20 h	0.1	6.3	13.9
3[a]	Starch	170 °C, 20 h	0.2	5.2	15.9
4[a]	Cellobiose	170 °C, 20 h	0.4	4.0	9.2

[a] Reaction conditions: 20 mg substrate, 5 mg CeO$_2$@B$_2$O$_3$, 5 mg γ-AlOOH, 1.7 mL ethanol, 0.3 mL DMSO; ND: not detected.

from 160 °C to 170 °C, the EMF production rate increased rapidly. In comparison, when the reaction temperature continued to increase to 180 °C, EMF yield decreased. The optimum temperature was 170 °C, the excessive temperature would backfire and form its by-product ethyl levulinate (EL), as shown in Fig. 5(c). Reaction time is another significant factor influencing the yield of EMF. At all temperatures, the yield of EMF increased gradually with the prolongation of the reaction time and then decreased after reaching the peak, which was caused by the side-reaction occurrence. These results demonstrate that similar to temperature, excessive time will also reduce the selectivity.

3.4. Effect of amount of DMSO on the conversion of glucose into EMF

In addition to catalyst loading, reaction temperature and time, a suitable solvent system is also vital for the efficient carbohydrates conversion into EMF. As an affordable solvent with good thermal stability and high polarity, DMSO has good application prospects in the catalytic conversion of carbohydrates to EMF. In order to enhance the selectivity and yield of EMF, the effect of solvent on EMF yield was studied by adjusting the ratio of DMSO and ethanol in solvent system. As indicated in Table 2, compared with pure ethanol as solvent, the addition of 0.3 mL and 0.5 mL DMSO can promote the conversion of glucose into
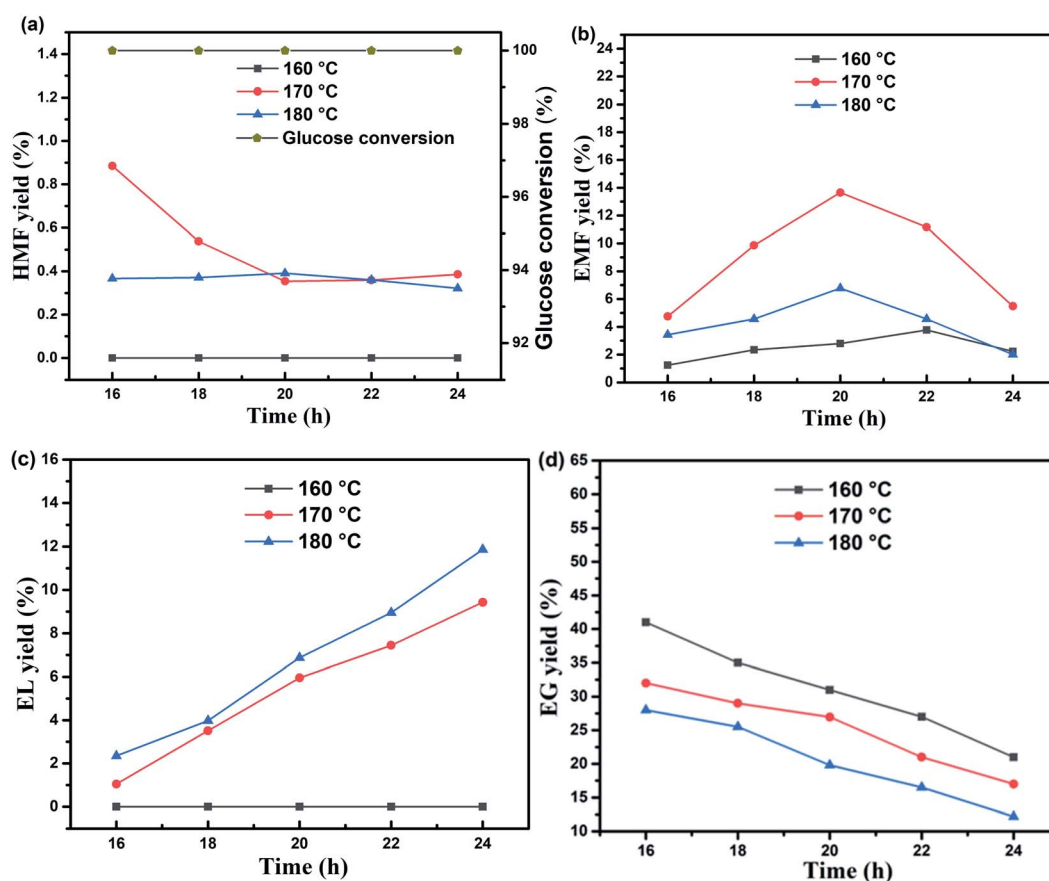

Fig. 5 Effect of reaction temperature and time on the conversion of glucose into EMF, (a) HMF yield, (b) EMF yield, (c) EL yield, (d) EG yield. Reaction conditions: 20 mg substrate, catalyst (5 mg CeO$_2$@B$_2$O$_3$, 5 mg γ-AlOOH), solvent (1.7 mL ethanol, 0.3 mL DMSO), 170 °C, 20 h.

Table 4 Comparison of various catalyst systems for the synthesis of EMF from glucose

Entry	Catalyst	glucose/catalyst mass ratio	Reaction conditions	EMF yield/%	References
1	γ-AlOOH, CeO₂@B₂O₃	2	170 °C, 20 h	27.7	This work
2	MIL-101SO₃H(100)	1.8	130 °C, 15 h	<10	29
3	OMC–SO₃H	1.8	140 °C, 24 h	0.9	49
4	B–H-beta (12.5)	1.5	125 °C, 11 h	16	32
5	PCP(Cr)–BA	2	140 °C, 22 h	23.1	50

EMF and EL. When the concentration of DMSO is further increased to 0.7 mL, the maximum yield of glucose reaction at 170 °C for 20 h is 27.7%. However, when the content of DMSO is further increased to 1.0 mL, the yield of EMF starts to decrease quickly to 17.6%. These results demonstrate that the addition of DMSO significantly affects the product distribution and promotes the formation of EMF until a specific concentration. This could be ascribed to the fact that the introduction of DMSO can help the dehydration reaction and prevent the polymerization of intermediate products and the side reactions.[9] Nonetheless, a high concentration of DMSO would reduce the relative content of ethanol in the solvent system, thus slowing down the etherification rate of intermediate HMF, which is not conducive to generating EMF.[45]

3.5. Study on the preparation of EMF from other carbohydrates

In order to further explore the scope of application of the catalytic system, other carbohydrates including sucrose, inulin, starch and cellobiose were involved as raw materials to produce EMF, and the results are summarized in Table 3. Under the reaction conditions of 170 °C and 20 h, the EMF yields of sucrose, inulin and starch were similar, which were 13.6%, 13.9% and 15.9%, respectively. These results indicate that the catalytic system can not only promote the etherification and dehydration reactions, but especially the high strength of Brønsted acidity contained in it can effectively promote the hydrolysis of glycosidic bonds.[46] In contrast, the yield of EMF obtained from cellobiose was lower at 9.2%. This is attributed to the good symmetry of cellobiose linked by β-1,4 glycosidic bonds, making its hydrolysis more difficult.[47] Moreover, most of the reported heterogeneous catalytic systems are not ideal for the alcoholysis of glucose dimer, and its depolymerization usually requires more stringent reaction conditions.[48] Simultaneously, the catalytic performance was compared with other heterogeneous solid acid systems, and the results were shown in Table 4. The substrate/catalyst mass ratio was used as a measure of the catalytic performance per unit mass of catalyst (average mass of γ-AlOOH and CeO₂@B₂O₃). The mass ratio of γ-AlOOH and CeO₂@B₂O₃ synergistic catalytic system is 2, which is higher than other catalytic systems, indicating that higher EMF yield and higher catalytic efficiency can be obtained with lower catalyst loading.

3.6. Reusability

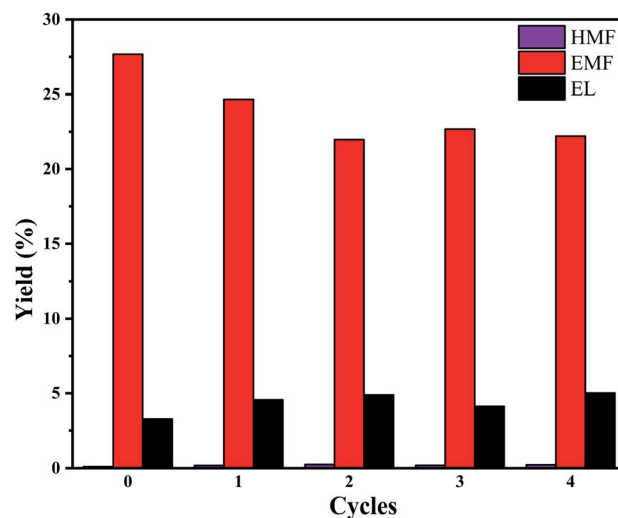The reusability and long-term stability of the heterogeneous catalysts are of great significance for EMF production in

Fig. 6 Recycling experiment of CeO₂@B₂O₃/γ-AlOOH. Reaction conditions: 20 mg glucose, catalyst (5 mg CeO₂@B₂O₃, 5 mg γ-AlOOH), solvent (1.3 mL ethanol, 0.7 mL DMSO), 170 °C, 20 h.

practical application. After the reaction was completed, the catalyst was separated from the mixture by centrifugation, washed with ethanol and deionized water for five consecutive times to remove the deposited carbonaceous products on the catalyst's surface, and then dried in a vacuum oven at 120 °C for 24 h. The as-separated catalysts were used directly for the next reusability experiment without further regeneration steps. The reusability study was conducted five times with glucose as raw material and the total reaction time of 100 hours. As can be seen from Fig. 6, during the first two rounds of reuse, the yield of EMF decreased slightly (~3.0%). Although there was a decline in the subsequent rounds, the fluctuation was not too high and the yield remained relatively stable.

4. Conclusions

In summary, this work proposed an alternative promising route for the heterogeneous catalytic preparation of EMF from carbohydrates. Specifically, the synergic catalytic system of solid acid catalysts CeO₂@B₂O₃ and γ-AlOOH was developed. When the amount of the two catalysts was the same as 5 mg (the distribution ratio of weak acid, medium-strong acid and strong acid was 1.00 : 9.18 : 11.76; the ratio of Brønsted acidity/Lewis acidity was 0.18), in ethanol/DMSO solvent system at 170 °C

reactions 20 h, catalyzed glucose into EMF, the highest yield was 27.7%. The synergy between strong, medium-strong and weak different acid sites and the synergy between Brønsted acidity and Lewis acidity together promote the cascade reaction of carbohydrate conversion to EMF. Moreover, the catalytic system for other glucose-based carbohydrates (sucrose, cellobiose, inulin, starch) synthesis of EMF yields were moderate (9.2–15.9%). In addition, the reusability experiment shows that the catalytic system has no apparent activity loss after repeated use five times without regeneration steps, and the separation process is facile and simple.

Conflicts of interest

There are no conflicts to declare.

Acknowledgements

References

1 C. García-Sancho, I. Fúnez-Núñez, R. Moreno-Tost, J. Santamaría-González, E. Pérez-Inestrosa, J. L. G. Fierro and P. Maireles-Torres, Beneficial effects of calcium chloride on glucose dehydration to 5-hydroxymethylfurfural in the presence of alumina as catalyst, *Appl. Catal., B*, 2017, **206**, 617–625, DOI: 10.1016/j.apcatb.2017.01.065.

2 Y. He, L. Zhang, Y. Liu, S. Yi, H. Yu, Y. Zhu and R. Sun, Sulfated complex metal oxides solid acids with dual Bronsted-Lewis acidic property for production of 5-ethoxymethylfurfural from biomass-derived carbohydrates, *Chem. Eng. J.*, 2022, **429**, 132279, DOI: 10.1016/j.cej.2021.132279.

3 Y. Jing, Y. Guo, Q. Xia, X. Liu and Y. Wang, Catalytic Production of Value-Added Chemicals and Liquid Fuels from Lignocellulosic Biomass, *Chem*, 2019, **5**, 2520–2546, DOI: 10.1016/j.chempr.2019.05.022.

4 Z. Yuan, Z. Zhang, J. Zheng and J. Lin, Efficient synthesis of promising liquid fuels 5-ethoxymethylfurfural from carbohydrates, *Fuel*, 2015, **150**, 236–242, DOI: 10.1016/j.fuel.2015.02.020.

5 M. Zuo, K. Le, Z. Li, Y. Jiang, X. Zeng, X. Tang, Y. Sun and L. Lin, Green process for production of 5-hydroxymethylfurfural from carbohydrates with high purity in deep eutectic solvents, *Ind. Crops Prod.*, 2017, **99**, 1–6, DOI: 10.1016/j.indcrop.2017.01.027.

6 Y.-Y. Bai, S. Su, S. Wang, B. Wang, R.-C. Sun, G. Song and L.-P. Xiao, Catalytic Conversion of Carbohydrates into 5-Ethoxymethylfurfural by a Magnetic Solid Acid Using γ-Valerolactone as a Co-Solvent, *Energy Technol.*, 2018, **6**, 1951–1958, DOI: 10.1002/ente.201800090.

7 B. S. Rao, D. D. Lakshmi, P. K. Kumari, P. Rajitha and N. Lingaiah, Dehydrative etherification of carbohydrates to 5-ethoxymethylfurfural over SBA-15-supported Sn-modified heteropolysilicate catalysts, *Sustainable Energy Fuels*, 2020, **4**, 3428–3437, DOI: 10.1039/d0se00509f.

8 B. Chen, G. Xu, Z. Zheng, D. Wang, C. Zou and C. Chang, Efficient conversion of corn stover into 5-ethoxymethylfurfural catalyzed by zeolite USY in ethanol/THF medium, *Ind. Crops Prod.*, 2019, **129**, 503–511, DOI: 10.1016/j.indcrop.2018.12.027.

9 G. Morales, M. Paniagua, J. A. Melero and J. Iglesias, Efficient production of 5-ethoxymethylfurfural from fructose by sulfonic mesostructured silica using DMSO as co-solvent, *Catal. Today*, 2017, **279**, 305–316, DOI: 10.1016/j.cattod.2016.02.016.

10 S. Alipour, H. Omidvarborna and D.-S. Kim, A review on synthesis of alkoxymethyl furfural, a biofuel candidate, *Renewable Sustainable Energy Rev.*, 2017, **71**, 908–926, DOI: 10.1016/j.rser.2016.12.118.

11 A. B. Gawade and G. D. Yadav, Microwave assisted synthesis of 5-ethoxymethylfurfural in one pot from d-fructose by using deep eutectic solvent as catalyst under mild condition, *Biomass Bioenergy*, 2018, **117**, 38–43, DOI: 10.1016/j.biombioe.2018.07.008.

12 Y. Bai, L. Wei, M. Yang, H. Chen, S. Holdren, G. Zhu, D. T. Tran, C. Yao, R. Sun, Y. Pan and D. Liu, Three-step cascade over a single catalyst: synthesis of 5-(ethoxymethyl) furfural from glucose over a hierarchical lamellar multi-functional zeolite catalyst, *J. Mater. Chem. A*, 2018, **6**, 7693–7705, DOI: 10.1039/c8ta01242c.

13 F. Yang, J. Tang, R. Ou, Z. Guo, S. Gao, Y. Wang, X. Wang, L. Chen and A. Yuan, Fully catalytic upgrading synthesis of 5-Ethoxymethylfurfural from biomass-derived 5-Hydroxymethylfurfural over recyclable layered-niobium-molybdate solid acid, *Appl. Catal., B*, 2019, **256**, 117786, DOI: 10.1016/j.apcatb.2019.117786.

14 G. Xu, B. Chen, Z. Zheng, K. Li and H. Tao, One-pot ethanolysis of carbohydrates to promising biofuels: 5-ethoxymethylfurfural and ethyl levulinate, *Asia-Pac. J. Chem. Eng.*, 2017, **12**, 527–535, DOI: 10.1002/apj.2095.

15 T. Chen, L. Peng, X. Yu and L. He, Magnetically recyclable cellulose-derived carbonaceous solid acid catalyzed the biofuel 5-ethoxymethylfurfural synthesis from renewable carbohydrates, *Fuel*, 2018, **219**, 344–352, DOI: 10.1016/j.fuel.2018.01.129.

16 H. Qu, B. Liu, G. Gao, Y. Ma, Y. Zhou, H. Zhou, L. Li, Y. Li and S. Liu, Metal-organic framework containing Brønsted acidity and Lewis acidity for efficient conversion glucose to levulinic acid, *Fuel Process. Technol.*, 2019, **193**, 1–6, DOI: 10.1016/j.fuproc.2019.04.035.

17 H. Xia, H. Hu, S. Xu, K. Xiao and S. Zuo, Catalytic conversion of glucose to 5-hydroxymethyfural over Fe/β zeolites with

extra-framework isolated Fe species in a biphasic reaction system, *Biomass Bioenergy*, 2018, **108**, 426–432, DOI: **10.1016/j.biombioe.2017.12.007**.

18 C. M. Lew, N. Rajabbeigi and M. Tsapatsis, One-Pot Synthesis of 5-(Ethoxymethyl)furfural from Glucose Using Sn-BEA and Amberlyst Catalysts, *Ind. Eng. Chem. Res.*, 2012, **51**, 5364–5366, DOI: **10.1021/ie2025536**.

19 H. Guo, A. Duereh, Y. Hiraga, X. Qi and R. L. Smith, Mechanism of Glucose Conversion into 5-Ethoxymethylfurfural in Ethanol with Hydrogen Sulfate Ionic Liquid Additives and a Lewis Acid Catalyst, *Energy Fuels*, 2018, **32**, 8411–8419, DOI: **10.1021/acs.energyfuels.8b00717**.

20 B. Xiang, Y. Wang, T. Qi, H.-Q. Yang and C.-W. Hu, Promotion catalytic role of ethanol on Brønsted acid for the sequential dehydration-etherification of fructose to 5-ethoxymethylfurfural, *J. Catal.*, 2017, **352**, 586–598, DOI: **10.1016/j.jcat.2017.06.031**.

21 Y. Yang, M. M. Abu-Omar and C. Hu, Heteropolyacid catalyzed conversion of fructose, sucrose, and inulin to 5-ethoxymethylfurfural, a liquid biofuel candidate, *Appl. Energy*, 2012, **99**, 80–84, DOI: **10.1016/j.apenergy.2012.04.049**.

22 G. Raveendra, A. Rajasekhar, M. Srinivas, P. S. Sai Prasad and N. Lingaiah, Selective etherification of hydroxymethylfurfural to biofuel additives over Cs containing silicotungstic acid catalysts, *Appl. Catal., A*, 2016, **520**, 105–113, DOI: **10.1016/j.apcata.2016.04.017**.

23 Y. Wen, Z. Yu, K. Li, H. Guo, Y. Dai and L. Yan, Fabrication of biobased heterogeneous solid Brønsted acid catalysts and their application on the synthesis of liquid biofuel 5-ethoxymethylfurfural from fructose, *Green Energy Environ.*, 2018, **3**, 384–391, DOI: **10.1016/j.gee.2018.07.003**.

24 H. Guo, A. Duereh, Y. Hiraga, T. M. Aida, X. Qi and R. L. Smith, Perfect recycle and mechanistic role of hydrogen sulfate ionic liquids as additive in ethanol for efficient conversion of carbohydrates into 5-ethoxymethylfurfural, *Chem. Eng. J.*, 2017, **323**, 287–294, DOI: **10.1016/j.cej.2017.04.111**.

25 H. Wang, T. Deng, Y. Wang, X. Cui, Y. Qi, X. Mu, X. Hou and Y. Zhu, Graphene oxide as a facile acid catalyst for the one-pot conversion of carbohydrates into 5-ethoxymethylfurfural, *Green Chem.*, 2013, **15**, 2379–2383, DOI: **10.1039/c3gc41109e**.

26 H. Li, K. S. Govind, R. Kotni, S. Shunmugavel, A. Riisager and S. Yang, Direct catalytic transformation of carbohydrates into 5-ethoxymethylfurfural with acid-base bifunctional hybrid nanospheres, *Energy Convers. Manage.*, 2014, **88**, 1245–1251, DOI: **10.1016/j.enconman.2014.03.037**.

27 Z. Zheng, C. Wang, Y. Chen, S. Wang, Q. Guo, C. Chang, H. Tao and G. Xu, One-pot efficient conversion of glucose into biofuel 5-ethoxymethylfurfural catalyzed by zeolite solid catalyst, *Biomass Convers. Biorefin.*, 2021, DOI: **10.1007/s13399-021-01660-1**.

28 B. Liu and Z. Zhang, One-pot conversion of carbohydrates into 5-ethoxymethylfurfural and ethyl d-glucopyranoside in ethanol catalyzed by a silica supported sulfonic acid catalyst, *RSC Adv.*, 2013, **3**, 12313–12319, DOI: **10.1039/C3RA41043A**.

29 X. Liu, H. Li, H. Pan, H. Zhang, S. Huang, K. Yang, W. Xue and S. Yang, Efficient catalytic conversion of carbohydrates into 5-ethoxymethylfurfural over MIL-101-based sulfated porous coordination polymers, *J. Energy Chem.*, 2016, **25**, 523–530, DOI: **10.1016/j.jechem.2016.01.015**.

30 L. di Bitonto, G. Antonopoulou, C. Braguglia, C. Campanale, A. Gallipoli, G. Lyberatos, I. Ntaikou and C. Pastore, Lewis-Bronsted acid catalysed ethanolysis of the organic fraction of municipal solid waste for efficient production of biofuels, *Bioresour. Technol.*, 2018, **266**, 297–305, DOI: **10.1016/j.biortech.2018.06.110**.

31 Y. Chen, L. Peng, J. Zhang and L. He, Synergy of $Al_2(SO_4)_3$ and H_3PO_4 in co-solvents converts starch to 5-ethoxymethylfurfural, *Catal. Commun.*, 2020, **137**, 105947, DOI: **10.1016/j.catcom.2020.105947**.

32 H. Li, S. Saravanamurugan, S. Yang and A. Riisager, Direct transformation of carbohydrates to the biofuel 5-ethoxymethylfurfural by solid acid catalysts, *Green Chem.*, 2016, **18**, 726–734, DOI: **10.1039/C5GC01043H**.

33 P. Lanzafame, D. M. Temi, S. Perathoner, G. Centi, A. Macario, A. Aloise and G. Giordano, Etherification of 5-hydroxymethyl-2-furfural (HMF) with ethanol to biodiesel components using mesoporous solid acidic catalysts, *Catal. Today*, 2011, **175**, 435–441, DOI: **10.1016/j.cattod.2011.05.008**.

34 X. Yu, X. Gao, L. Peng, L. He and J. Zhang, Intensified 5-Ethoxymethylfurfural Production from Biomass Components over Aluminum-Based Mixed-Acid Catalyst in Co-Solvent Medium, *ChemistrySelect*, 2018, **3**, 13391–13399, DOI: **10.1002/slct.201803059**.

35 C. Tao, L. Peng, J. Zhang and L. He, Al-modified heteropolyacid facilitates alkyl levulinate production from cellulose and lignocellulosic biomass: Kinetics and mechanism studies, *Fuel Process. Technol.*, 2021, **213**, 106709, DOI: **10.1016/j.fuproc.2020.106709**.

36 A. Takagaki, J. C. Jung and S. Hayashi, Solid Lewis acidity of boehmite γ-AlO(OH) and its catalytic activity for transformation of sugars in water, *RSC Adv.*, 2014, **4**, 43785–43791, DOI: **10.1039/C4RA08061K**.

37 B. Han, P. Zhao, R. He, T. Wu and Y. Wu, Catalytic Conversion of Glucose to 5-Hydroxymethyfurfural Over B_2O_3 Supported Solid Acids Catalysts, *Waste Biomass Valorization*, 2018, **9**, 2181–2190, DOI: **10.1007/s12649-017-9971-4**.

38 X. Zhou, J. Zhang, Y. Ma, H. Tian, Y. Wang, Y. Li, L. Jiang and Q. Cui, The solvothermal synthesis of γ-AlOOH nanoflakes and their compression behaviors under high pressures, *RSC Adv.*, 2017, 7, 4904–4911, DOI: **10.1039/C6RA27571K**.

39 L. Y. Zhu, X. Q. Wang, G. H. Zhang, Q. Ren and D. Xu, Structural characterization and photocatalytic activity of $B_2O_3/ZrO_2–TiO_2$ mesoporous fibers, *Appl. Catal., B*, 2011, **103**, 428–435, DOI: **10.1016/j.apcatb.2011.02.006**.

40 L. Zhang, L. Zhang, G. Xu, C. Zhang, X. Li, Z. Sun and D. Jia, Low-temperature CO oxidation over CeO_2 and $CeO_2@Co_3O_4$

core–shell microspheres, *New J. Chem.*, 2017, **41**, 13418–13424, DOI: **10.1039/C7NJ02542D**.

41 H. Zhang, P. Li, W. Cui, C. Liu, S. Wang, S. Zheng and Y. Zhang, Synthesis of nanostructured γ-AlOOH and its accelerating behavior on the thermal decomposition of AP, *RSC Adv.*, 2016, **6**, 27235–27241, DOI: **10.1039/C5RA27838D**.

42 O. S. Bezrkovnyi, M. Vorokhta, M. Małecka, W. Mista and L. Kepinski, NAP-XPS study of $Eu^{3+} \rightarrow Eu^{2+}$ and $Ce^{4+} \rightarrow Ce^{3+}$ reduction in $Au/Ce_{0.80}Eu_{0.20}O_2$ catalyst, *Catal. Commun.*, 2020, **135**, 105875, DOI: **10.1016/j.catcom.2019.105875**.

43 K. Wu, D. Liu, H. Duan, X. Jin, S. Yin and W. Yao, Green and facile synthesis of cube-like γ-AlOOH and its usage for fabricating Mg stabilized Na-β''-Al_2O_3 powders, *Ceram. Int.*, 2020, **46**, 22367–22372, DOI: **10.1016/j.ceramint.2020.05.318**.

44 H. Li, Z. Fang, J. Luo and S. Yang, Direct conversion of biomass components to the biofuel methyl levulinate catalyzed by acid-base bifunctional zirconia-zeolites, *Appl. Catal., B*, 2017, **200**, 182–191, DOI: **10.1016/j.apcatb.2016.07.007**.

45 H. Wang, T. Deng, Y. Wang, Y. Qi, X. Hou and Y. Zhu, Efficient catalytic system for the conversion of fructose into 5-ethoxymethylfurfural, *Bioresour. Technol.*, 2013, **136**, 394–400, DOI: **10.1016/j.biortech.2013.02.110**.

46 L. Jiang, L. Zhou, J. Chao, H. Zhao, T. Lu, Y. Su, X. Yang and J. Xu, Direct catalytic conversion of carbohydrates to methyl levulinate: Synergy of solid Brønsted acid and Lewis acid, *Appl. Catal., B*, 2018, **220**, 589–596, DOI: **10.1016/j.apcatb.2017.08.072**.

47 K. Nakajima and M. Hara, Amorphous Carbon with SO_3H Groups as a Solid Brønsted Acid Catalyst, *ACS Catal.*, 2012, **2**, 1296–1304, DOI: **10.1021/cs300103k**.

48 Y. He, L. Zhang, Y. Liu, S. Yi, H. Yu, Y. Zhu and R. Sun, Sulfated complex metal oxides solid acids with dual Brønsted-Lewis acidic property for production of 5-ethoxymethylfurfural from biomass-derived carbohydrates, *Chem. Eng. J.*, 2022, **429**, 132279, DOI: **10.1016/j.cej.2021.132279**.

49 J. Wang, Z. Zhang, S. Jin and X. Shen, Efficient conversion of carbohydrates into 5-hydroxylmethylfurfan and 5-ethoxymethylfurfural over sufonic acid-functionalized mesoporous carbon catalyst, *Fuel*, 2017, **192**, 102–107, DOI: **10.1016/j.fuel.2016.12.027**.

50 L. Zhang, Y. Liu, R. Sun and S. Yi, Sulfonic acid-functionalized PCP(Cr) catalysts with Cr^{3+} and -SO_3H sites for 5-ethoxymethylfurfural production from glucose, *RSC Adv.*, 2021, **11**(54), 33969–33979, DOI: **10.1039/d1ra05103b**.